SEMARAK ILMU PUBLISHING

Semarak International Journal of Nanotechnology

Journal homepage:
https://semarakilmu.com.my/journals/index.php/sijn/index

Flow and Heat Transfer Analysis of Hybrid Nanofluid over a Rotating Disk with a Uniform Shrinking Rate in the Radial Direction: Dual Solutions

Rusya Iryanti Yahaya[1,*], Norihan Md Arifin[1,2], Ioan Pop[3], Fadzilah Md Ali[1,2], Siti Suzilliana Putri Mohamed Isa[1,4]

[1] Institute for Mathematical Research, Universiti Putra Malaysia, 43400 UPM Serdang, Selangor, Malaysia
[2] Department of Mathematics and Statistics, Universiti Putra Malaysia, 43400 UPM Serdang, Selangor, Malaysia
[3] Department of Mathematics, Babeş-Bolyai University, 400084 Cluj-Napoca, Romania
[4] Centre of Foundation Studies For Agricultural Science, Universiti Putra Malaysia, 43400 UPM Serdang, Selangor, Malaysia

ARTICLE INFO

Article history:
Received : 14 March 2024
Received in revised form : 5 April 2024
Accepted : 5 May 2024
Available online : 10 June 2024

Keywords:
Uniform shrinking rate; hybrid nanofluid; injection; dual solutions; stability analysis

ABSTRACT

Rotating machinery, gas turbine rotators, and air cleaning equipment are some industrial and electronic applications of hybrid nanofluids as heat transfer fluids. Considering these potential applications, the axisymmetric flow of a hybrid nanofluid towards a permeable rotating disk with a uniform shrinking rate is analysed in the current study. Nonlinear ordinary differential equations and boundary conditions are generated, using Von Kármán's transformations, from the governing partial differential equations and boundary conditions. Then, a sophisticated bvp4c solver containing finite difference code is utilized for solving the boundary value problem numerically. Following the discovery of dual solutions, stability analysis is performed, and only the first solution is stable. Besides that, the magnitude of the local skin friction coefficient is found to increase with the rise of shrinking and injection parameters. However, the augmentation of the shrinking and injection parameters reduces and enhances the local Nusselt number. Meanwhile, the enhancement of injection parameter is observed to reduce the hybrid nanofluid's momentum and thermal boundary layer thickness.

1. Introduction

Two or more distinct nanoparticles dispersed in a base fluid create a hybrid nanofluid. Many years ago, attempts to find a more efficient and cost-saving heat transfer fluid were executed by Maxwell [1] and Masuda *et al.,* [2]. Conventional fluids have a limitation of low heat transfer performance owing to the small surface-to-volume ratio available for heat transfer. Both of these studies suggested the incorporation of solid particles and ultra-fine particles into conventional fluid (e.g., water, ethylene glycol, engine oil, and toluene). It was proven that the thermal conductivity of the fluid improves, but the sedimentation of these particles clogged flow passages. Choi and Eastman [3] then overcame this problem by introducing nanofluid produced from the dispersion of metallic

* *Corresponding author.*
E-mail address: rusyairyanti@gmail.com

particles with an average size of 10nm. The nanofluid has more advantages regarding better heat transfer performance and stability. Later, researchers analysed hybrid nanofluids. The suspension of dissimilar nanoparticles, for example, metal oxide nanoparticles of Al_2O_3, CuO, ZnO, or TiO_2 with metallic nanoparticles of Cu, Zn, Ag, or Ni, into the conventional heat transfer fluid is predicted to create a fluid with improved thermophysical properties [4]. Besides combining metal oxide with metallic nanoparticles, hybrid nanofluid can also be synthesized by combining carbon nanotubes and carbides. Like nanofluid, hybrid nanofluid has diverse potential applications as the working fluid in manufacturing processes, nuclear cooling systems, drug delivery systems (biomedical field), chemical engineering processes, car radiators, and domestic refrigerators [5, 6]. The published works by Nabil *et al.,* [7], Eshgarf *et al.,* [8], and Ukueje *et al.,* [9] provide further reading on hybrid nanofluids.

Before realizing the usage of hybrid nanofluid in real-life applications, researchers did rapid studies, either experimentally or theoretically, to understand this fluid's flow and thermal behaviors. The researchers in fluid dynamics conducted various studies to analyze the flow of hybrid nanofluids over different solid boundaries and prescribed conditions. Ghadikolaei *et al.,* [10] explored the magnetohydrodynamics (MHD) flow of a Carreau hybrid nanofluid over a rotating cone. The hybrid nanofluid consists of TiO_2 and CuO nanoparticles dispersed in an ethylene glycol-water mixture. The increase in viscosity variation parameter enhanced the velocity profiles, but the opposite occurred for the increasing values of Weissenberg and Hartman numbers. Meanwhile, the increase in shape factors enhanced the local Nusselt number related to heat transfer rate. Dinarvand *et al.,* [11] concurred with this observation for the Cu-CuO/blood flows at the stagnation point over a porous stretching sheet. Similarly, Khan *et al.,* [12] found that platelet-shaped nanoparticles perform more efficiently than brick- and cylindrical-shaped nanoparticles. Besides that, the local Sherwood number related to the mass transfer rate increased due to chemical reactions and activation energy in the TiO_2-Cu/H_2O flow through a stretching sheet. Meanwhile, Ahmad and Nadeem [13] discussed the ion slip effects on the combined free and forced convection flows of carbon nanotubes hybrid nanofluid across a stretching sheet. The ion slip effect enhanced the temperature and horizontal velocity profiles. Next, Waini *et al.,* [14] investigated the thermophoresis and Brownian motion in the Al_2O_3-Cu/H_2O flow past a moving thin needle. The increase in thermophoresis and Brownian motion parameters showed a contrasting effect on the nanoparticle concentration. The effects of Joule heating on the hybrid nanofluid flow over a contracting cylinder with suction were scrutinized by Khashi'ie *et al.,* [15]. Then, Benkhedda *et al.,* [16] evaluated the flows of Ag-TiO_2/H_2O and TiO_2/H_2O through a horizontal pipe. This investigation concluded that the friction factor of the hybrid nanofluid is more significant than that of the nanofluid. Thus, extra pumping power is needed for hybrid nanofluid flow compared to the nanofluid. Tulu and Ibrahim [17] then discussed the mixed convection flow of MWCNTs-Al_2O_3/engine oil hybrid nanofluid over a spinning cone. In this flow problem, the Nusselt number decreased when the variable thermal conductivity parameter increased. The numerical computation of hybrid nanofluid flow across a contracting/expanding sheet in the studies by Mousavi *et al.,* [18] and Yahaya and Arifin [19] produced dual solutions. These solutions were found in the shrinking case with suction, and the stability analysis identified that only one of the dual solutions was stable. Some recent studies on hybrid nanofluid were conducted by Nayan *et al.,* [20], Roy and Pop [21], Mahabaleshwar *et al.,* [22], Asghar *et al.,* [23], Mahesh *et al.,* [24], Patel *et al.,* [25], and Yahaya *et al.,* [26].

The first study of rotating-disk flow was by Von Kármán [27]. He presented the Navier-Stokes equations for this problem and introduced the famous transformations to reduce the equations into a system of ordinary differential equations. The problem is then solved using the momentum integral method. Cochran [28] then presented the asymptotic solution for the flow problem. Ackroyd [29] discussed the effects of suction and injection toward the steady flow over a rotating disk. Later, Attia

[30] examined these effects towards the unsteady flow with a magnetic field. In these studies, the disk was assumed to be permeable to allow suction and injection to occur at the disk surface. Attia [30] observed a more significant intensification of magnetic field effects on the flow with injection than suction. Takhar *et al.,* [31] expanded the research by introducing the energy equation together with the Navier-Stokes equations. It was discovered that an increase in the magnetic field decreases the heat transfer rate and surface shear stress in the radial direction while increasing it in the tangential direction. Then, Attia [32] studied the MHD flow and heat transfer of non-Newtonian fluid past a permeable rotating disk. In contrast to the non-Newtonian parameter, the magnetic field has been observed to stabilize the flow. The nanofluid flow over a permeable rotating disk was then examined by Rashidi *et al.,* [33] with the effects of entropy generation and magnetic field. The decrement in nanoparticle volume fraction, magnetic field, and suction parameters minimizes the entropy generation. Turkyilmazoglu [34] considered five different water-based nanofluids (i.e., Cu, CuO, Ag, Al_2O_3, and TiO_2) and found that more torque was needed to preserve the steady rotation of the disk when Ag, Cu, and CuO nanoparticles were used. Then, Yin *et al.,* [35] discussed the nanofluid flow across a rotating disk with radial expansion. The enhancement of the stretching parameter was detected to cause the increment of local skin friction and heat transfer rate together with the axial and radial velocities. Hayat *et al.,* [36] and Alghamdi [37] then scrutinized the nanofluid flow across a rotating disk with a stagnation point and mixed convection, respectively. In the meantime, Naganthran *et al.,* [38] and Sarkar and Sahoo [39] obtained dual solutions for the flow problem involving a shrinking/stretching rotating disk. Gamachu and Ibrahim [40] analyzed the hybrid nanofluid's rotating-disk flow with the findings of diminishing concentration and temperature distributions by the increase in the nanoparticle volume fraction. Meanwhile, Waqas *et al.,* [41], Kumar and Mondal [42], and Kumar and Sharma [43] studied the radiative flow of a hybrid nanofluid past a rotating disk. The fluid's temperature profile increased due to the thermal radiation parameter. The unsteady MHD rotating-disk flow of hybrid ferrofluid was examined by Waini *et al.* [44]. Pandey and Das [45] studied the hybrid nanofluid flow over a rotating, stretching disk with magnetic field effects. Recent investigations on hybrid nanofluid and ternary hybrid nanofluid flow over a rotating disk with velocity slips and nonlinear convection were published by Algehyne *et al.,* [46] and Ullah *et al.,* [47]. Singla *et al.,* [48] then conducted an intriguing comparative investigation on mono, hybrid, and ternary nanofluids flow between two rotating disks.

The classical rotating-disk flow has many practical applications, such as for rotating machinery, gas turbine rotators, thermal power generating systems, electronic apparatus, chemical processes, oceanography, the geothermal industry, medical machines, computer storage devices, and air cleaning equipment [40]. Thus, incorporating the rotating-disk flow problem with a hybrid nanofluid as the working fluid (heat transfer fluid) is relevant for many real-life applications. It is found that the study on hybrid nanofluid flow past a permeable, rotating, shrinking disk has not been considered by other researchers. Therefore, the current study will analyze the steady flow of Al_2O_3-Cu/H_2O hybrid nanofluid over a permeable rotating disk. The disk is assumed to shrink in the radial direction with a uniform shrinking rate. The mathematical formulation for the flow problem will be described in the next section. Besides that, the familiar Von Kármán's transformations will be applied to convert the governing equations and boundary conditions into a set of ordinary differential equations. Then, MATLAB's bvp4c solver will be used to execute all numerical computations using the finite difference code in this solver. Dual solutions generated by the numerical computation at specified values of injection and shrinking parameters distinguish this research from others. In order to determine the physically realizable and stable solution, it is necessary to execute a stability analysis. The current study will provide crucial information on the hybrid nanofluid behaviors in the rotating-disk flow with injection and uniform shrinking rate.

2. Mathematical Formulation

Consider a hybrid nanofluid's flow and heat transfer over a rotating disk with an angular velocity Ω and a uniform shrinking velocity $u_w(r)$ in the radial direction r. As depicted in Figure 1, (r, φ, z) are the cylindrical coordinates with the (r, φ)- axes measured along the plane of the disk, and the z −axis is normal to it; the flow occupies the domain $z \geq 0$. The flow is axially symmetric; thus, $\partial/\partial\varphi = 0$ for all variables. It is presumed that the mass flux velocity is w_w and the disk's surface temperature is T_w, while T_∞ is the working fluid's temperature with $T_w > T_\infty$ for a hot disk. The working fluid is a water-based hybrid nanofluid (H_2O) that contains alumina (Al_2O_3) and copper (Cu) nanoparticles. Moreover, it is presumed that the base fluid and the suspended nanoparticles are in thermal equilibrium and that the nanoparticles have a uniform size and shape and are also in a thermal equilibrium state.

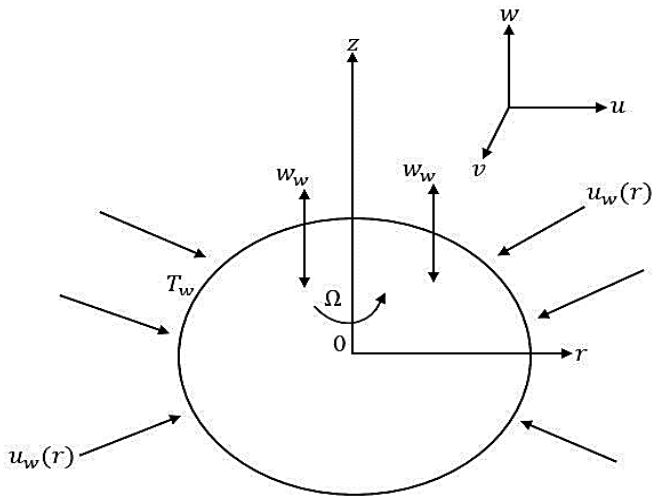

Fig. 1. The flow problem's physical representation and coordinate system

Under these assumptions, the continuity, momentum, and energy equations are as follows [34], [35], [49]:

$$\frac{\partial u}{\partial r} + \frac{u}{r} + \frac{\partial w}{\partial z} = 0, \tag{1}$$

$$u\frac{\partial u}{\partial r} + w\frac{\partial u}{\partial z} = \frac{\mu_{hnf}}{\rho_{hnf}}\left[\frac{1}{r}\frac{\partial}{\partial r}\left(r\frac{\partial u}{\partial r}\right) - \frac{u}{r^2} + \frac{\partial^2 u}{\partial z^2}\right] + \frac{v^2}{r}, \tag{2}$$

$$u\frac{\partial v}{\partial r} + w\frac{\partial v}{\partial z} = \frac{\mu_{hnf}}{\rho_{hnf}}\left[\frac{1}{r}\frac{\partial}{\partial r}\left(r\frac{\partial v}{\partial r}\right) - \frac{v}{r^2} + \frac{\partial^2 v}{\partial z^2}\right] - \frac{u v}{r}, \tag{3}$$

$$u\frac{\partial w}{\partial r} + w\frac{\partial w}{\partial z} = \frac{\mu_{hnf}}{\rho_{hnf}}\left[\frac{1}{r}\frac{\partial}{\partial r}\left(r\frac{\partial w}{\partial r}\right) + \frac{\partial^2 w}{\partial z^2}\right] - \frac{1}{\rho_{hnf}}\frac{\partial p}{\partial z}, \tag{4}$$

$$u\frac{\partial T}{\partial r} + w\frac{\partial T}{\partial z} = \frac{k_{hnf}}{(\rho C_p)_{hnf}}\left[\frac{1}{r}\frac{\partial}{\partial r}\left(r\frac{\partial T}{\partial r}\right) + \frac{\partial^2 T}{\partial z^2}\right], \tag{5}$$

subject to the boundary conditions:

$$\left.\begin{array}{c} u = u_w(r) = a\,r,\ \ v = v_w(r) = \Omega\,r,\ \ w = w_w,\ T = T_w \quad \text{at} \quad z = 0 \\ u = u_e \to 0,\ v = v_e \to 0,\ T \to T_\infty \quad \text{as} \quad z \to \infty \end{array}\right\}. \tag{6}$$

Here, (u, v, w) are velocities along (r, φ, z)- axes of the disk, p is the pressure, T is the temperature, and a is a shrinking constant of dimension $(\text{time})^{-1}$. Further,

$$\left.\begin{array}{c} \mu_{hnf} = \mu_{bf}\left(1 - \phi_{Al_2O_3} - \phi_{Cu}\right)^{-2.5} \\ \rho_{hnf} = \phi_{Al_2O_3}\rho_{Al_2O_3} + \phi_{Cu}\rho_{Cu} + \left(1 - \phi_{hnf}\right)\rho_{bf} \\ \dfrac{k_{hnf}}{k_{bf}} = \left\{\dfrac{\phi_{Al_2O_3}k_{Al_2O_3} + \phi_{Cu}k_{Cu}}{\phi_{hnf}} + 2k_{bf} + 2\left(\phi_{Al_2O_3}k_{Al_2O_3} + \phi_{Cu}k_{Cu}\right) - 2\left(\phi_{hnf}\right)k_{bf}\right\} \times \\ \left\{\dfrac{\phi_{Al_2O_3}k_{Al_2O_3} + \phi_{Cu}k_{Cu}}{\phi_{hnf}} + 2k_{bf} - \left(\phi_{Al_2O_3}k_{Al_2O_3} + \phi_{Cu}k_{Cu}\right) + \left(\phi_{hnf}\right)k_{bf}\right\}^{-1} \\ \left(\rho C_p\right)_{hnf} = \phi_{Al_2O_3}\left(\rho C_p\right)_{Al_2O_3} + \phi_{Cu}\left(\rho C_p\right)_{Cu} + \left(1 - \phi_{hnf}\right)\left(\rho C_p\right)_{bf} \\ \text{and } \phi_{hnf} = \phi_{Al_2O_3} + \phi_{Cu} \end{array}\right\}, \tag{7}$$

are the correlations from Takabi and Salehi [50] and Devi and Devi [49] for dynamic viscosity (μ_{hnf}), density (ρ_{hnf}), thermal conductivity (k_{hnf}), and heat capacity ($\left(\rho C_p\right)_{hnf}$) of the hybrid nanofluid. Meanwhile, ϕ represents the volume fraction of nanoparticles, and the suffix bf refers to the base fluid. By referring to Oztop and Abu-Nada [51] and Khashi'ie *et al.,* [52], the physical characteristics of the nanoparticles and base fluid are given in Table 1.

Table 1
Thermophysical characteristics of water, alumina, and copper

Physical Properties	H_2O (water)	Al_2O_3 (alumina)	Cu (copper)
$\rho\ (kg/m^3)$	997.1	3970	8933
$C_p\ (J/kg\ K)$	4179	765	385
$k\ (W/mK)$	0.613	40	401
$\mu\ (kg/ms\ )$	8.90×10^{-4}	-	-

To solve the governing equations (1) to (6), we take the following similarity transformations [27]:

$$u = \Omega\,r f(\eta), \quad v = \Omega\,r g(\eta), \qquad w = \sqrt{\Omega\,\nu_{bf}}\,h(\eta), \quad \theta(\eta) = \frac{T\ -\ T_\infty}{T_w\ -\ T_\infty}, \quad \eta = z\sqrt{\frac{\Omega}{\nu_{bf}}},$$
$$p - p_\infty = 2\,\mu_{bf}\,\Omega\,p(\eta). \tag{8}$$

Thus, we have:

$$w_w = \sqrt{\Omega\,\nu_{bf}}\,S, \tag{9}$$

where S is the constant mass flux parameter with $S < 0$ for injection and $S > 0$ for suction, meanwhile, ν_{bf} is the kinematic viscosity of water.

Ordinary (similarity) differential equations and boundary conditions are obtained after substituting (8) into Eq. (1)-(6):

$$2\,f + h' = 0, \tag{10}$$

$$Af'' - hf' - f^2 + \ g^2 = 0, \tag{11}$$

$$Ag'' - h\ g' - 2fg = 0, \tag{12}$$

$$B\theta'' - Prh\,\theta' = 0, \tag{13}$$

$$\left.\begin{matrix} g(\eta) = 1, \quad f(\eta) = \beta, \ \ h(\eta) = S, \ \ \theta(\eta) = 1 \ \text{at} \quad \eta = 0 \\ g(\eta) \to 0, \ \ f(\eta) \to 0, \ \ \theta(\eta) \to 0 \quad \text{as} \quad \eta \to \infty \end{matrix}\right\}, \tag{14}$$

where the prime denotes differentiation with respect to η, $Pr = (\mu\ C_p)_{bf}/k_{bf}$ implies the Prandtl number, and $\beta = a/\Omega$ represents the shrinking parameter that measures the ratio of radial shrink to swirl with $\beta = 0$ corresponding to the non-shrinking case. In the equations, $A = \frac{\mu_{hnf}/\mu_{bf}}{\rho_{hnf}/\rho_{bf}}$ and $B = \frac{k_{hnf}/k_{bf}}{(\rho\ C_p)_{hnf}/(\rho\ C_p)_{bf}}$.

The quantities of practical interest are the skin friction coefficient C_f and the local Nusselt number Nu_r, which are defined as:

$$C_f = \frac{\mu_{hnf}\sqrt{\tau_{wr}^2 + \tau_{w\varphi}^2}}{\rho_{bf}\ (\Omega\ r)^2}\ , Nu_r = \frac{r\ k_{nf}}{k_{bf}\ (T_w - T_\infty)}\left(-\frac{\partial\ T}{\partial\ z}\right)_{z=0}, \tag{15}$$

where τ_{wr} and $\tau_{w\varphi}$ are the radial and tangential shear stress at $z = 0$, respectively:

$$\tau_{wr} = \left(\frac{\partial\ u}{\partial\ z} + \frac{\partial\ w}{\partial\ \varphi}\right)_{z=0}, \ \ \tau_{w\varphi} = \left(\frac{\partial\ v}{\partial\ z} + \frac{1}{r}\ \frac{\partial\ w}{\partial\ \varphi}\right)_{z=0}. \tag{16}$$

Using (8), (15) and (16), we obtain:

$$Re_r^{1/2} C_f = \frac{\mu_{hnf}}{\mu_{bf}}\sqrt{[f'(0)]^2 + \ [g'(0)]^2}, \quad Re_r^{-1/2} Nu_r = -\ \frac{k_{hnf}}{k_{bf}}\theta'(0). \tag{17}$$

We noticed that for $\phi_{hnf} = 0$ (classical viscous fluid), the boundary value problem (i.e., Eqs. (10)-(14)) reduces to those by Rashidi *et al.,* [33] and Turkyilmazoglu [34]. Thus, the numerical computation and solutions to the current problem (at $\phi_{hnf} = 0$) can be validated and compared with these studies. The present study will conduct the numerical analysis using MATLAB's bvp4c solver.

3. Stability Analysis

Several studies have disclosed the presence of multiple solutions for problems involving the fluid flow over a shrinking surface with suction/injection [18], [38], [53]. Since the current problem deals with the flow over a permeable shrinking disk, it is interesting to perform stability analysis to

determine the stability and significance of the obtained solutions. Time-dependent or unsteady equations for the current problem are introduced as:

$$\frac{\partial u}{\partial r}+\frac{u}{r}+\frac{\partial w}{\partial z}=0, \tag{18}$$

$$u\frac{\partial u}{\partial r}+w\frac{\partial u}{\partial z}+\frac{\partial u}{\partial t}=\frac{\mu_{hnf}}{\rho_{hnf}}\left[\frac{1}{r}\frac{\partial}{\partial r}\left(r\frac{\partial u}{\partial r}\right)-\frac{u}{r^2}+\frac{\partial^2 u}{\partial z^2}\right]+\frac{v^2}{r}, \tag{19}$$

$$u\frac{\partial v}{\partial r}+w\frac{\partial v}{\partial z}+\frac{\partial v}{\partial t}=\frac{\mu_{hnf}}{\rho_{hnf}}\left[\frac{1}{r}\frac{\partial}{\partial r}\left(r\frac{\partial v}{\partial r}\right)-\frac{v}{r^2}+\frac{\partial^2 v}{\partial z^2}\right]-\frac{u\,v}{r}, \tag{20}$$

$$u\frac{\partial w}{\partial r}+w\frac{\partial w}{\partial z}+\frac{\partial w}{\partial t}=\frac{\mu_{hnf}}{\rho_{hnf}}\left[\frac{1}{r}\frac{\partial}{\partial r}\left(r\frac{\partial w}{\partial r}\right)+\frac{\partial^2 w}{\partial z^2}\right]-\frac{1}{\rho_{hnf}}\frac{\partial p}{\partial z}, \tag{21}$$

$$u\frac{\partial T}{\partial r}+w\frac{\partial T}{\partial z}+\frac{\partial T}{\partial t}=\frac{k_{hnf}}{(\rho C_p)_{hnf}}\left[\frac{1}{r}\frac{\partial}{\partial r}\left(r\frac{\partial T}{\partial r}\right)+\frac{\partial^2 T}{\partial z^2}\right], \tag{22}$$

and these equations can be simplified using the following similarity transformations:

$$u=\Omega\, r f(\eta,\tau),\quad v=\Omega\, r g(\eta,\tau),\ w=\sqrt{\Omega\,\nu_{bf}}\,h(\eta,\tau),\quad \theta(\eta,\tau)=\frac{T-T_\infty}{T_w-T_\infty},$$
$$p-p_\infty=2\,\mu_{bf}\,\Omega\,p(\eta,\tau),\qquad \eta=z\sqrt{\frac{\Omega}{\nu_{bf}}},\qquad \tau=\Omega t, \tag{23}$$

with τ as the dimensionless time variable containing time t. Thus, substituting (23) into Eqs. (18)-(22) produces:

$$2f+\frac{\partial h}{\partial \eta}=0, \tag{24}$$

$$A\frac{\partial^2 f}{\partial \eta^2}-f^2+g^2-h\frac{\partial f}{\partial \eta}-\frac{\partial f}{\partial \tau}=0, \tag{25}$$

$$A\frac{\partial^2 g}{\partial \eta^2}-h\frac{\partial g}{\partial \eta}-2fg-\frac{\partial g}{\partial \tau}=0, \tag{26}$$

$$B\frac{\partial^2 \theta}{\partial \eta^2}-Prh\frac{\partial \theta}{\partial \eta}-Pr\frac{\partial \theta}{\partial \tau}=0, \tag{27}$$

subjected to the boundary conditions of:

$$\left.\begin{aligned} &g(\eta,\tau)=1,\ \ f(\eta,\tau)=\beta,\ \ h(\eta,\tau)=S,\ \ \theta(\eta,\tau)=1 \quad \text{at}\quad \eta=0\\ &g(\eta,\tau)\to 0,\quad f(\eta,\tau)\to 0,\ \ \theta(\eta,\tau)\to 0 \quad \text{as}\quad \eta\to\infty \end{aligned}\right\}. \tag{28}$$

In accordance with Weidman *et al.,* [54] and Roşca and Pop [55], the following perturbation functions are introduced:

$$\left.\begin{aligned} h(\eta,\tau) &= h_0(\eta) + e^{-\gamma\tau}\, H(\eta,\tau) \\ f(\eta,\tau) &= f_0(\eta) + e^{-\gamma\tau}\, F(\eta,\tau) \\ g(\eta,\tau) &= g_0(\eta) + e^{-\gamma\tau}\, G(\eta,\tau) \\ \theta(\eta,\tau) &= \theta_0(\eta) + e^{-\gamma\tau}\, M(\eta,\tau) \end{aligned}\right\}, \tag{29}$$

that contain exponential functions to describe the development of disturbance in the steady flow solutions $f = f_0(\eta)$, $g = g_0(\eta)$, $h = h_0(\eta)$, and $\theta = \theta_0(\eta)$ where $f_0 \gg F(\eta,\tau)$, $g_0 \gg G(\eta,\tau)$, $h_0 \gg H(\eta,\tau)$, and $\theta_0 \gg M(\eta,\tau)$. The eigenvalue problem with γ as the unknown eigenvalue is obtained after substituting (29) into (24)-(28). The solution is said to be stable and meaningful if there exists an initial decay of disturbance that is represented by the positive smallest eigenvalue γ_1. Otherwise, the solution is unstable. The initial decay or growth of disturbance can be determined by setting the value of $\tau = 0$. Thus, $F(\eta) = F_0(\eta)$, $G(\eta) = G_0(\eta)$, $H(\eta) = H_0(\eta)$, and $M(\eta) = M_0(\eta)$. The values of γ can be computed by solving the following linearized eigenvalue problem using the bvp4c solver in MATLAB:

$$2\,F_0 + H_0' = 0, \tag{30}$$

$$AF_0'' - 2f_0F_0 + 2g_0G_0 - h_0F_0' - H_0f_0' + \gamma F_0 = 0, \tag{31}$$

$$AG_0'' - h_0G_0' - H_0g_0' - 2f_0G_0 - 2F_0g_0 + \gamma G_0 = 0, \tag{32}$$

$$BM_0'' - Prh_0M_0' - PrH_0\theta_0' + Pr\gamma M_0 = 0, \tag{33}$$

$$\left.\begin{aligned} &F_0(0) = 0,\ \ G_0(0) = 0,\ \ H_0(0) = 0,\ \ M_0(0) = 0 \\ &F_0(\eta) \to 0,\quad G_0(\eta) \to 0,\ M_0(\eta) \to 0 \quad \text{as} \quad \eta \to \infty \end{aligned}\right\}. \tag{34}$$

The possible range of γ (i.e., $\gamma_1 < \gamma_2 < \gamma_3 < \gamma_4 < \cdots$) can be achieved by relaxing one of the free stream boundary conditions in (34). In this study, $F_0(\eta) \to 0$ is relaxed to form $F_0'(0) = 1$ so that the smallest eigenvalue γ_1 can be attained from the numerical computation of Eqs. (30)-(34). Wahid *et al.,* [53] briefly described the method of solutions using the bvp4c solver.

4. Results and Discussion

The boundary value problem (10)-(14) is solved using the bvp4c solver in MATLAB 9.3 R2017b. Before any calculations are made, the mathematical formulation and method are checked by comparing them with other published studies. The numerical results reported in the studies by Rashidi *et al.,* [33] and Turkyilmazoglu [34] are calculated using the shooting and spectral Chebyshev collocation methods, respectively. To compare the results, we have set $\phi_{Al_2O_3} = \phi_{Cu} = S = \beta = 0$ and $Pr = 6.2$ to match the previous studies. The comparison of these results is displayed in Table 2. As demonstrated in this table, the present results, computed using the bvp4c solver, are well-agreed with the results from the previous studies. Thus, it grants confidence in the formulation and method employed in the current study.

Table 2
Comparison of results with other published studies

	Present study	Turkyilmazoglu [29]	Rashidi *et al.,* [28]
$f'(0)$	0.51023	0.51023262	0.510186
$-g'(0)$	0.61592	0.61592201	0.61589
$-\theta'(0)$	0.93388	0.93387794	-

The bvp4c solver contains a solinit function that requires an initial guess as an input. Multiple solutions are found when various initial guesses generate dissimilar solutions. In the present study, two solutions are generated by the solver, which brings about stability analysis of solutions. Incorporating injection effects with the selected values of other controlling parameters contributed to dual solutions in this flow problem. Meanwhile, the results of the stability analysis are presented in Table 3. It can be declared that only the first solution is stable and meaningful, as the smallest eigenvalue γ_1 is observed to be positive. Hence, the upcoming discussion will focus on the first solution.

Table 3
Smallest eigenvalues γ_1 when $\phi_{Al_2O_3} = \phi_{Cu} = 0.02$, $\beta = -0.3$, and $Pr = 6.2$

S	γ_1	
	First solution	Second solution
-0.4	0.35906	-0.60018
-0.5	0.36024	-0.67025
-0.6	0.36317	-0.68629

The local Nusselt number ($Re_r^{-1/2}Nu_r$) and skin friction coefficient ($Re_r^{1/2}C_f$) are shown in Table 4 for various values of shrinking and constant mass flux parameters. In this study, dual solutions are obtained when considering the shrinking case (i.e., $\beta < 0$) with injection (i.e., $S < 0$). The values of $Re_r^{1/2}C_f$ are seen to increase with the magnitude of the shrinking parameter. Similar behavior is observed as the injection parameter's magnitude increases. However, the values of $Re_r^{-1/2}Nu_r$, which corresponds to the heat transfer rate, reduce as the shrinking parameter increases; this may be due to the reduction of the hot shrinking sheet area available for heat transfer. Nevertheless, the augmentation of the injection parameter promotes heat transfer and raises the local Nusselt number.

Table 4
Values of $Re_r^{1/2}C_f$ and $Re_r^{-1/2}Nu_r$ for $\phi_{Al_2O_3} = \phi_{Cu} = 0.02$ and $Pr = 6.2$

S	β	$Re_r^{1/2}C_f$		$Re_r^{-1/2}Nu_r$	
		First solution	Second solution	First solution	Second solution
-0.4	-0.3	1.07378	6.51569	1.96347	0.00000
-0.5		1.10798	5.30981	2.54554	0.00000
	-0.2	1.09444	5.00381	2.84540	0.00000
	-0.4	1.14619	5.58995	2.19863	0.00000
-0.6	-0.3	1.14483	4.49070	3.15579	0.00000

Next, Figure 2 illustrates the effect of the shrinking parameter on the velocity profiles of the hybrid nanofluid. The increment in the magnitude of the shrinking parameter affects the radial velocity profile at the region near and far from the disk differently. As shown in Figure 2 (a), the increase in $|\beta|$ lowers the radial velocity profile of the hybrid nanofluid near the disk, contrary to the behavior

observed some distance from the disk. As the disk shrinks in the radial direction, the no-slip condition causes the radial velocity of the hybrid nanofluid near the disk to decrease as the shrinking parameter increases. After some distance away, the shrinking effects of the disk towards the radial velocity of the fluid diminishes. However, the tangential and axial velocity profiles show an increasing behavior with $|\beta|$ at both locations near and far from the shrinking disk, as depicted in Figures 2(b) and 2(c). Similarly, as observed in Figure 3, the rise in $|\beta|$ also raises the temperature profile. The thermal boundary layer thickens with $|\beta|$, which causes the reduction of the temperature gradient (i.e., $-\theta'(0)$) and local Nusselt number, $Re_r^{-1/2}Nu_r\left(=-\frac{k_{hnf}}{k_{bf}}\theta'(0)\right)$ (see Table 4).

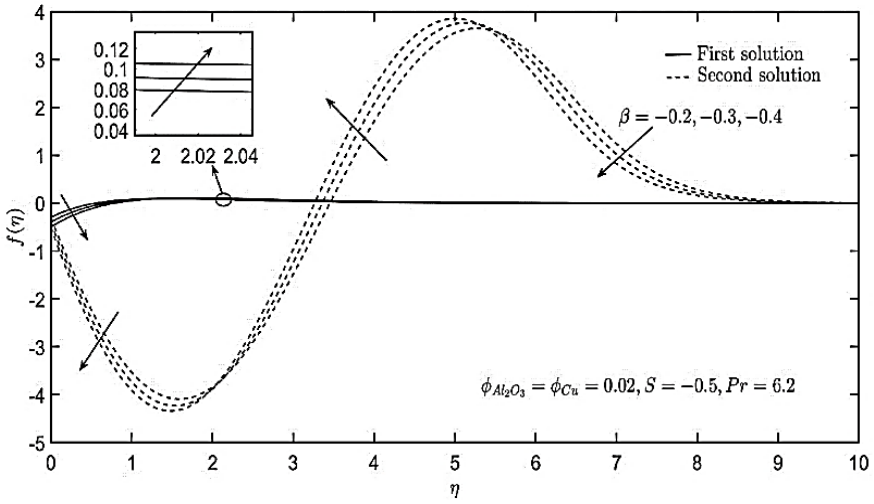

(a)

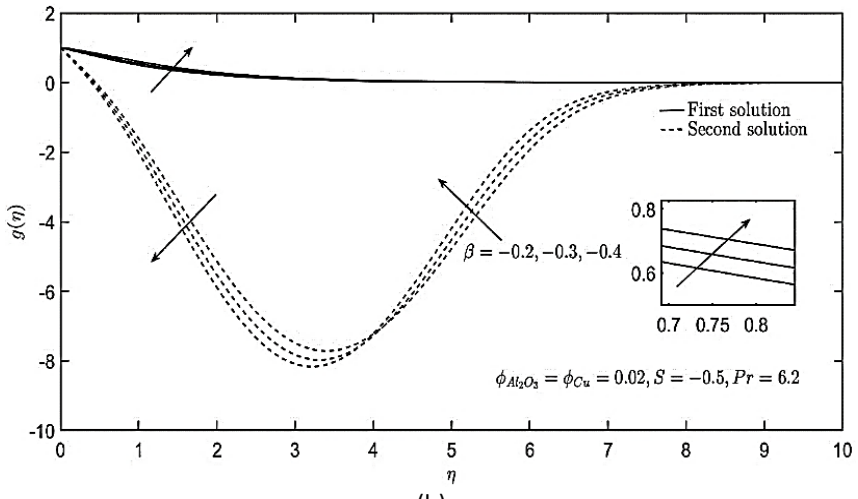

(b)

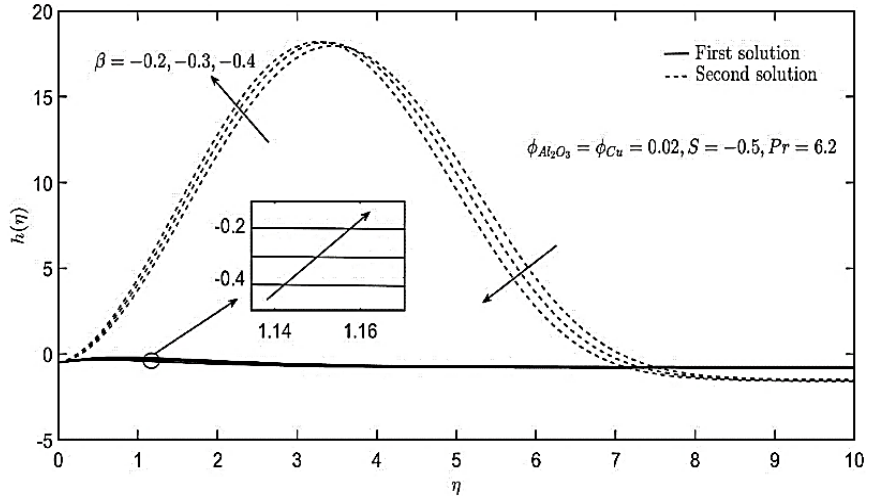

(c)

Fig. 2. Profiles of (a) radial, (b) tangential, and (c) axial velocities with different values of the shrinking parameter

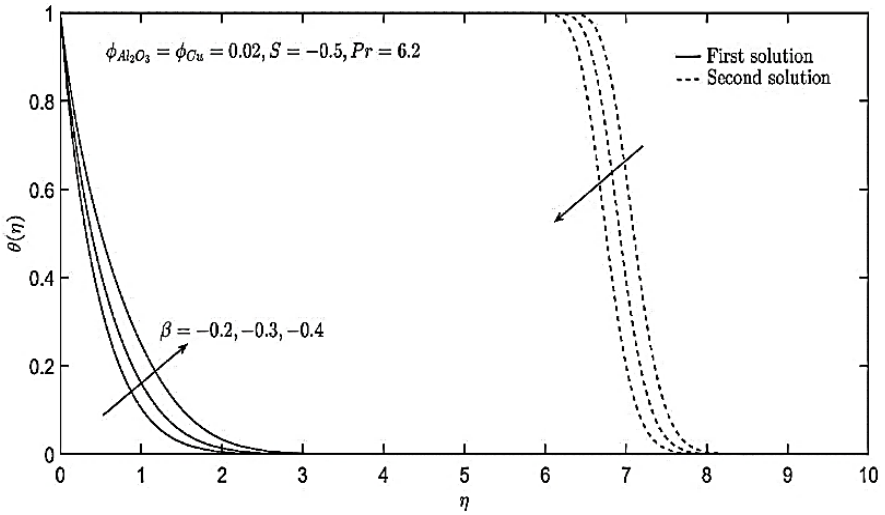

Fig. 3. Temperature profile with various values of the shrinking parameter

Then, the impacts of the injection parameter $(S < 0)$ on the velocity profiles are presented in Figure 4. In Figure 4(a), the radial velocity increases with $|S|$. The opposite seems to occur for the tangential and axial velocity profiles in Figures 4(b) and 4(c), respectively. Nonetheless, the momentum boundary layers in the radial, tangential, and axial directions are noticed to shrink as the magnitude of the injection parameter increases. The temperature profile shows the same observation (see Figure 5). As the cold hybrid nanofluid is injected through the disk, the temperature profile of the fluid decreases as the injection parameter increases. The augmentation of the injection parameter then diminishes the thermal boundary layer. Consequently, it enhances the temperature gradient that boosts the heat transfer rate and Nusselt number, as obtained in Table 4.

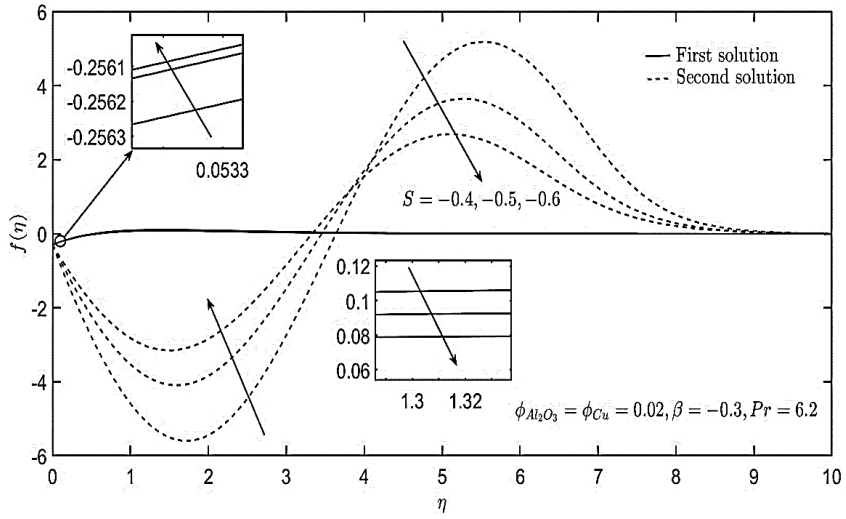

(a)

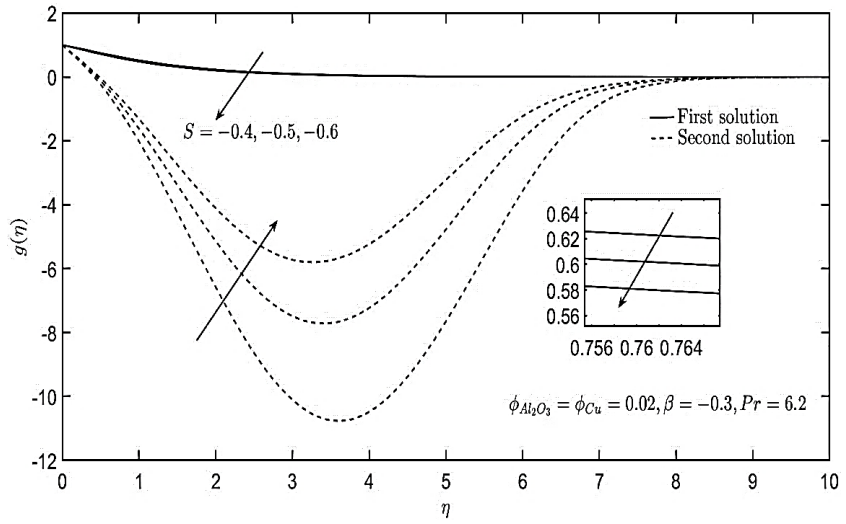

(b)

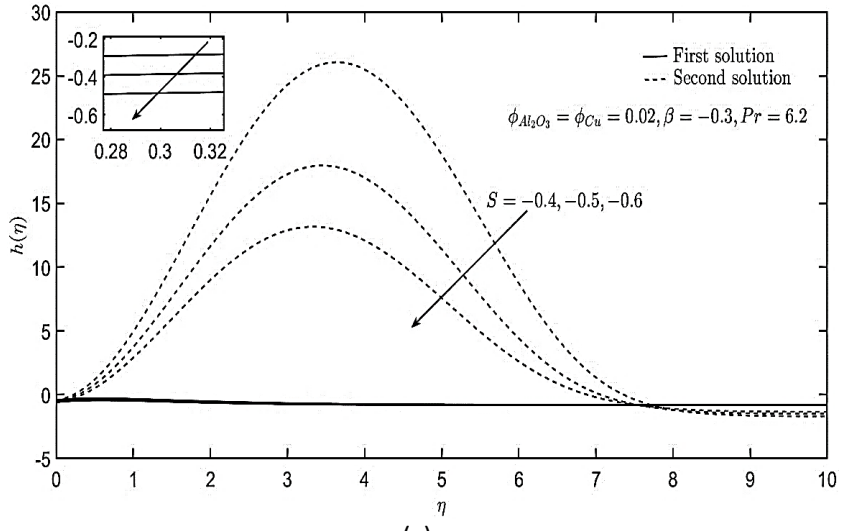

(c)

Fig. 4. Profiles of (a) Radial, (b) Tangential and (c) Axial velocities with different values of injection parameter

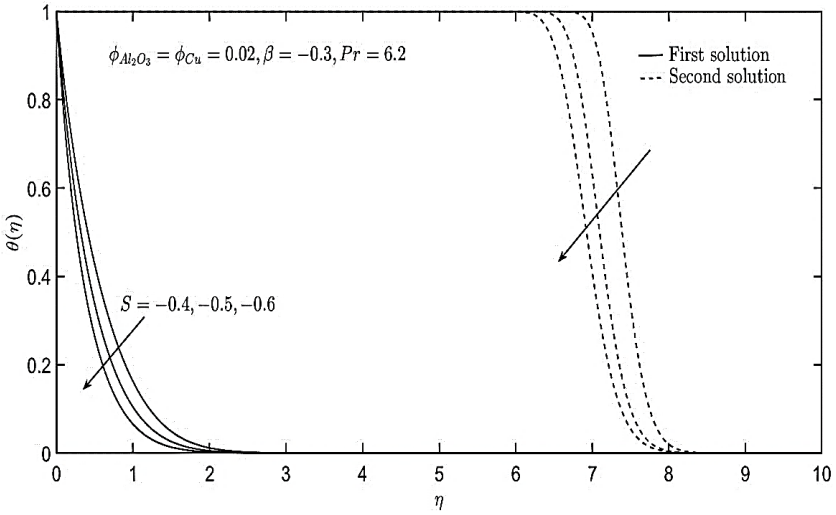

Fig. 5. Temperature profile with various values of injection parameter

5. Conclusion

The current study analysed the flow of Al_2O_3-Cu/H_2O over a rotating disk with a uniform shrinking rate and injection. A mathematical formulation consisting of differential equations and boundary conditions is solved numerically using the bvp4c solver in MATLAB. The findings can be summarized as follows:

i. Dual solutions are found, but only the first solution is stable, as verified through the stability analysis.
ii. The augmentation of the shrinking parameter enhances the local skin friction coefficient but lowers the local Nusselt number.
iii. In contrast, the increase in injection parameter raises the local Nusselt number and skin friction coefficient.

Since the current study is limited to the flow of a hybrid nanofluid, a comparative analysis for mono, hybrid, and ternary nanofluids can be done for future works. Other conditions, such as velocity slip, suction, zero mass flux, and thermal radiation, can also be considered and incorporated into the mathematical formulation of the flow problem.

Acknowledgement
This research was funded by a grant from Universiti Putra Malaysia (GP-GPB 9711400).

References
[1] Maxwell, James Clerk. *A treatise on electricity and magnetism*. Vol. 1. Oxford: Clarendon Press, 1873.
[2] Masuda, Hidetoshi, Akira Ebata, Kazunari Teramae, and Nobuo Hishinuma. "Alteration of Thermal Conductivity and Viscosity of Liquid by Dispersing Ultra-Fine Particles. Dispersion of Al2O3, SiO2 and TiO2 Ultra-Fine Particles." *Netsu Bussei* 7, no. 4 (1993): 227-233. https://doi.org/10.2963/jjtp.7.227
[3] Choi, S. US, and Jeffrey A. Eastman. *Enhancing thermal conductivity of fluids with nanoparticles*. No. ANL/MSD/CP-84938; CONF-951135-29. Argonne National Lab.(ANL), Argonne, IL (United States), 1995.
[4] Takabi, Behrouz, Amir Mirza Gheitaghy, and Pedram Tazraei. "Hybrid water-based suspension of Al2O3 and Cu nanoparticles on laminar convection effectiveness." *Journal of Thermophysics and Heat Transfer* 30, no. 3 (2016): 523-532. https://doi.org/10.2514/1.T4756

[5] Sundar, L. Syam, Korada Viswanatha Sharma, Manoj K. Singh, and A. C. M. Sousa. "Hybrid nanofluids preparation, thermal properties, heat transfer and friction factor–a review." *Renewable and Sustainable Energy Reviews* 68 (2017): 185-198. https://doi.org/10.1016/j.rser.2016.09.108

[6] Sulochana, C., and S. R. Aparna. "Unsteady magnetohydrodynamic radiative liquid thin film flow of hybrid nanofluid with thermophoresis and Brownian motion." *Multidiscipline Modeling in Materials and Structures* 16, no. 4 (2019): 811-834. https://doi.org/10.1108/MMMS-08-2019-0160

[7] Nabil, M. F., W. H. Azmi, K. A. Hamid, N. N. M. Zawawi, G. Priyandoko, and R. Mamat. "Thermo-physical properties of hybrid nanofluids and hybrid nanolubricants: a comprehensive review on performance." *International Communications in Heat and Mass Transfer* 83 (2017): 30-39. https://doi.org/10.1016/j.icheatmasstransfer.2017.03.008

[8] Eshgarf, Hamed, Rasool Kalbasi, Akbar Maleki, Mostafa Safdari Shadloo, and Arash Karimipour. "A review on the properties, preparation, models and stability of hybrid nanofluids to optimize energy consumption." *Journal of Thermal Analysis and Calorimetry* 144 (2021): 1959-1983. https://doi.org/10.1007/s10973-020-09998-w

[9] Ukueje, Wisdom Etabiese, Fidelis Ibiang Abam, and Anthony Obi. "A perspective review on thermal conductivity of hybrid nanofluids and their application in automobile radiator cooling." *Journal of Nanotechnology* 2022 (2022). https://doi.org/10.1155/2022/2187932

[10] Ghadikolaei, S. S., Kh Hosseinzadeh, and D. D. Ganji. "Investigation on ethylene glycol-water mixture fluid suspend by hybrid nanoparticles (TiO2-CuO) over rotating cone with considering nanoparticles shape factor." *Journal of Molecular Liquids* 272 (2018): 226-236. https://doi.org/10.1016/j.molliq.2018.09.084

[11] Dinarvand, Saeed, Mohammadreza Nademi Rostami, Rassoul Dinarvand, and Ioan Pop. "Improvement of drug delivery micro-circulatory system with a novel pattern of CuO-Cu/blood hybrid nanofluid flow towards a porous stretching sheet." *International Journal of Numerical Methods for Heat & Fluid Flow* 29, no. 11 (2019): 4408-4429. https://doi.org/10.1108/HFF-01-2019-0083

[12] Khan, M. Ijaz, Sohail A. Khan, T. Hayat, M. Imran Khan, and A. Alsaedi. "Arrhenius activation energy impact in binary chemically reactive flow of TiO 2-Cu-H 2 O hybrid nanomaterial." *International Journal of Chemical Reactor Engineering* 17, no. 3 (2019): 20180183. https://doi.org/10.1515/ijcre-2018-0183

[13] Ahmad, Shafiq, and Sohail Nadeem. "Analysis of activation energy and its impact on hybrid nanofluid in the presence of Hall and ion slip currents." *Applied Nanoscience* 10 (2020): 5315-5330. https://doi.org/10.1007/s13204-020-01334-w

[14] Waini, Iskandar, Anuar Ishak, and Ioan Pop. "Hybrid nanofluid flow past a permeable moving thin needle." *Mathematics* 8, no. 4 (2020): 612. https://doi.org/10.3390/math8040612

[15] Khashi'ie, Najiyah Safwa, Norihan Md Arifin, Ioan Pop, and Nur Syahirah Wahid. "Flow and heat transfer of hybrid nanofluid over a permeable shrinking cylinder with Joule heating: a comparative analysis." *Alexandria Engineering Journal* 59, no. 3 (2020): 1787-1798. https://doi.org/10.1016/j.aej.2020.04.048

[16] Benkhedda, Mohammed, Toufik Boufendi, Tahar Tayebi, and Ali J. Chamkha. "Convective heat transfer performance of hybrid nanofluid in a horizontal pipe considering nanoparticles shapes effect." *Journal of Thermal analysis and Calorimetry* 140, no. 1 (2020): 411-425. https://doi.org/10.1007/s10973-019-08836-y

[17] Tulu, Ayele, and Wubshet Ibrahim. "Mixed convection hybrid nanofluids flow of MWCNTs–Al2O3/engine oil over a spinning cone with variable viscosity and thermal conductivity." *Heat Transfer* 50, no. 4 (2021): 3776-3799. https://doi.org/10.1002/htj.22051

[18] Mousavi, Seyed Mahdi, Mohammadreza Nademi Rostami, Mohammad Yousefi, Saeed Dinarvand, Ioan Pop, and Mikhail A. Sheremet. "Dual solutions for Casson hybrid nanofluid flow due to a stretching/shrinking sheet: A new combination of theoretical and experimental models." *Chinese Journal of Physics* 71 (2021): 574-588. https://doi.org/10.1016/j.cjph.2021.04.004

[19] Yahaya, Rusya Iryanti, and Norihan Md Arifin. "Magnetohydrodynamic Flow Of Hybrid Ag-Cuo/H 2 O Nanofluid Past A Stretching/Shrinking Porous Plate With Viscous-Ohmic Dissipation And Heat Generation/Absorption." *Magnetohydrodynamics (0024-998X)* 57, no. 3 (2021). https://doi.org/10.22364/mhd.57.3.7

[20] Nayan, Asmahani, Nur Izzatie Farhana Ahmad Fauzan, Mohd Rijal Ilias, Shahida Farhan Zakaria, and Noor Hafizah Zainal Aznam. "Aligned magnetohydrodynamics (MHD) flow of hybrid nanofluid over a vertical plate through porous medium." *Journal of Advanced Research in Fluid Mechanics and Thermal Sciences* 92, no. 1 (2022): 51-64. https://doi.org/10.37934/arfmts.92.1.5164

[21] Roy, Nepal Chandra, and Ioan Pop. "Heat and mass transfer of a hybrid nanofluid flow with binary chemical reaction over a permeable shrinking surface." *Chinese Journal of Physics* 76 (2022): 283-298. https://doi.org/10.1016/j.cjph.2021.10.041

[22] Mahabaleshwar, U. S., A. B. Vishalakshi, and Helge I. Andersson. "Hybrid nanofluid flow past a stretching/shrinking sheet with thermal radiation and mass transpiration." *Chinese Journal of Physics* 75 (2022): 152-168. https://doi.org/10.1016/j.cjph.2021.12.014
[23] Asghar, Adnan, Liaquat Ali Lund, Zahir Shah, Narcisa Vrinceanu, Wejdan Deebani, and Meshal Shutaywi. "Effect of thermal radiation on three-dimensional magnetized rotating flow of a hybrid nanofluid." *Nanomaterials* 12, no. 9 (2022): 1566. https://doi.org/10.3390/nano12091566
[24] Mahesh, R., U. S. Mahabaleshwar, PN Vinay Kumar, Hakan F. Öztop, and Nidal Abu-Hamdeh. "Impact of radiation on the MHD couple stress hybrid nanofluid flow over a porous sheet with viscous dissipation." *Results in Engineering* 17 (2023): 100905. https://doi.org/10.1016/j.rineng.2023.100905
[25] Patel, Vijay K., Jigisha U. Pandya, and Manoj R. Patel. "Testing the influence of TiO2− Ag/water on hybrid nanofluid MHD flow with effect of radiation and slip conditions over exponentially stretching & shrinking sheets." *Journal of Magnetism and Magnetic Materials* 572 (2023): 170591. https://doi.org/10.1016/j.jmmm.2023.170591
[26] Yahaya, Rusya Iryanti, Norihan Md Arifin, Ioan Pop, Fadzilah Md Ali, and Siti Suzilliana Putri Mohamed Isa. "Dual solutions for the oblique stagnation-point flow of hybrid nanofluid towards a shrinking surface: Effects of suction." *Chinese Journal of Physics* 81 (2023): 193-205. https://doi.org/10.1016/j.cjph.2022.12.004
[27] Kármán, Th V. "Über laminare und turbulente Reibung." *ZAMM-Journal of Applied Mathematics and Mechanics/Zeitschrift für Angewandte Mathematik und Mechanik* 1, no. 4 (1921): 233-252. https://doi.org/10.1002/zamm.19210010401
[28] Cochran, W. G. "The flow due to a rotating disc." In *Mathematical proceedings of the Cambridge philosophical society*, vol. 30, no. 3, pp. 365-375. Cambridge University Press, 1934. https://doi.org/10.1017/S0305004100012561
[29] Ackroyd, J. A. D. "On the steady flow produced by a rotating disc with either surface suction or injection." *Journal of Engineering Mathematics* 12, no. 3 (1978): 207-220. https://doi.org/10.1007/BF00036459
[30] Attia, Hazem Ali. "Unsteady MHD flow near a rotating porous disk with uniform suction or injection." *Fluid Dynamics Research* 23, no. 5 (1998): 283. https://doi.org/10.1016/S0169-5983(98)80011-7
[31] Takhar, Harmindar S., Ashok K. Singh, and Girishwar Nath. "Unsteady MHD flow and heat transfer on a rotating disk in an ambient fluid." *International journal of thermal sciences* 41, no. 2 (2002): 147-155. https://doi.org/10.1016/S1290-0729(01)01292-3
[32] Attia, Hazem A. "Rotating disk flow and heat transfer of a conducting non-Newtonian fluid with suction-injection and ohmic heating." *Journal of the Brazilian Society of Mechanical Sciences and Engineering* 29 (2007): 168-173. https://doi.org/10.1590/S1678-58782007000200006
[33] Rashidi, M. M., S. Abelman, and N. Freidooni Mehr. "Entropy generation in steady MHD flow due to a rotating porous disk in a nanofluid." *International journal of Heat and Mass transfer* 62 (2013): 515-525. https://doi.org/10.1016/j.ijheatmasstransfer.2013.03.004
[34] Turkyilmazoglu, Mustafa. "Nanofluid flow and heat transfer due to a rotating disk." *Computers & Fluids* 94 (2014): 139-146. https://doi.org/10.1016/j.compfluid.2014.02.009
[35] Yin, Chenguang, Liancun Zheng, Chaoli Zhang, and Xinxin Zhang. "Flow and heat transfer of nanofluids over a rotating disk with uniform stretching rate in the radial direction." *Propulsion and Power Research* 6, no. 1 (2017): 25-30. https://doi.org/10.1016/j.jppr.2017.01.004
[36] Hayat, Tasawar, Madiha Rashid, Muhammad Ijaz Khan, and Ahmed Alsaedi. "Melting heat transfer and induced magnetic field effects on flow of water based nanofluid over a rotating disk with variable thickness." *Results in Physics* 9 (2018): 1618-1630. https://doi.org/10.1016/j.rinp.2018.04.054
[37] Alghamdi, Metib. "Significance of Arrhenius activation energy and binary chemical reaction in mixed convection flow of nanofluid due to a rotating disk." *Coatings* 10, no. 1 (2020): 86. https://doi.org/10.3390/coatings10010086
[38] Naganthran, Kohilavani, Meraj Mustafa, Ammar Mushtaq, and Roslinda Nazar. "Dual solutions for fluid flow over a stretching/shrinking rotating disk subject to variable fluid properties." *Physica A: Statistical Mechanics and Its Applications* 556 (2020): 124773. https://doi.org/10.1016/j.physa.2020.124773
[39] Sarkar, G. M., and B. Sahoo. "On dual solutions of the unsteady MHD flow on a stretchable rotating disk with heat transfer and a linear temporal stability analysis." *European Journal of Mechanics-B/Fluids* 85 (2021): 149-157. https://doi.org/10.1016/j.euromechflu.2020.09.010
[40] Gamachu, Dachasa, and Wubshet Ibrahim. "Mixed convection flow of viscoelastic Ag-Al2O3/water hybrid nanofluid past a rotating disk." *Physica Scripta* 96, no. 12 (2021): 125205. https://doi.org/10.1088/1402-4896/ac1a89
[41] Waqas, Hassan, Umar Farooq, Rabia Naseem, Sajjad Hussain, and Metib Alghamdi. "Impact of MHD radiative flow of hybrid nanofluid over a rotating disk." *Case Studies in Thermal Engineering* 26 (2021): 101015. https://doi.org/10.1016/j.csite.2021.101015

[42] Kumar, Mahesh, and Pranab Kumar Mondal. "Irreversibility analysis of hybrid nanofluid flow over a rotating disk: Effect of thermal radiation and magnetic field." *Colloids and Surfaces A: Physicochemical and Engineering Aspects* 635 (2022): 128077. https://doi.org/10.1016/j.colsurfa.2021.128077

[43] Kumar, Sanjay, and Kushal Sharma. "Entropy optimized radiative heat transfer of hybrid nanofluid over vertical moving rotating disk with partial slip." *Chinese Journal of Physics* 77 (2022): 861-873. https://doi.org/10.1016/j.cjph.2022.03.006

[44] Waini, Iskandar, Najiyah Safwa Khashi'ie, Abdul Rahman Mohd Kasim, Nurul Amira Zainal, Khairum Bin Hamzah, Norihan Md Arifin, and Ioan Pop. "Unsteady magnetohydrodynamics (MHD) flow of hybrid ferrofluid due to a rotating disk." *Mathematics* 10, no. 10 (2022): 1658. https://doi.org/10.3390/math10101658

[45] Pandey, Amit Kumar, and Abhijit Das. "Rotationally symmetric hybrid-nanofluid flow over a stretchable rotating disk." *European Journal of Mechanics-B/Fluids* 101 (2023): 227-245. https://doi.org/10.1016/j.euromechflu.2023.06.001

[46] Algehyne, Ebrahem A., Izharul Haq, Zehba Raizah, Fuad S. Alduais, Anwar Saeed, and Ahmed M. Galal. "Heat transport phenomenon of the MHD water-based hybrid nanofluid flow over a rotating disk with velocity slips." *International Journal of Modern Physics B* 38, no. 07 (2024): 2450100. https://doi.org/10.1142/S0217979224501005

[47] Ullah, Arbab Zaki, Xin Guo, Taza Gul, Ishtiaq Ali, Anwar Saeed, and Ahmed M. Galal. "Thin film flow of the ternary hybrid nanofluid over a rotating disk under the influence of magnetic field due to nonlinear convection." *Journal of Magnetism and Magnetic Materials* 573 (2023): 170673. https://doi.org/10.1016/j.jmmm.2023.170673

[48] Singla, Tanvi, Sapna Sharma, and B. Kumar. "Significance of radiant-energy and multiple slips on convective flow of mono, binary and ternary hybrid nanofluids: A comparative study." *International Journal of Modern Physics B* 38, no. 07 (2024): 2450093. https://doi.org/10.1142/S0217979224500930

[49] Devi, SP Anjali, and S. Suriya Uma Devi. "Numerical investigation of hydromagnetic hybrid Cu–Al2O3/water nanofluid flow over a permeable stretching sheet with suction." *International Journal of Nonlinear Sciences and Numerical Simulation* 17, no. 5 (2016): 249-257. https://doi.org/10.1515/ijnsns-2016-0037

[50] Takabi, Behrouz, and Saeed Salehi. "Augmentation of the heat transfer performance of a sinusoidal corrugated enclosure by employing hybrid nanofluid." *Advances in Mechanical Engineering* 6 (2014): 147059. https://doi.org/10.1155/2014/147059

[51] Oztop, Hakan F., and Eiyad Abu-Nada. "Numerical study of natural convection in partially heated rectangular enclosures filled with nanofluids." *International journal of heat and fluid flow* 29, no. 5 (2008): 1326-1336. https://doi.org/10.1016/j.ijheatfluidflow.2008.04.009

[52] Khashi'ie, Najiyah Safwa, Iskandar Waini, Norihan Md Arifin, and Ioan Pop. "Unsteady squeezing flow of Cu-Al2O3/water hybrid nanofluid in a horizontal channel with magnetic field." *Scientific reports* 11, no. 1 (2021): 14128. https://doi.org/10.1038/s41598-021-93644-4

[53] Wahid, Nur Syahirah, Nor Aliza Abd Rahmin, Norihan Md Arifin, Najiyah Safwa Khashi'ie, Ioan Pop, Norfifah Bachok, and Mohd Ezad Hafidz Hafidzuddin. "Radiative Blasius Hybrid Nanofluid Flow Over a Permeable Moving Surface with Convective Boundary Condition." *Journal of Advanced Research in Fluid Mechanics and Thermal Sciences* 100, no. 3 (2022): 115-132. https://doi.org/10.37934/arfmts.100.3.115132

[54] Weidman, P. D., D. G. Kubitschek, and A. M. J. Davis. "The effect of transpiration on self-similar boundary layer flow over moving surfaces." *International journal of engineering science* 44, no. 11-12 (2006): 730-737. https://doi.org/10.1016/j.ijengsci.2006.04.005

[55] Roşca, Alin V., and Ioan Pop. "Flow and heat transfer over a vertical permeable stretching/shrinking sheet with a second order slip." *International Journal of Heat and Mass Transfer* 60 (2013): 355-364. https://doi.org/10.1016/j.ijheatmasstransfer.2012.12.028